J Nanostruct 15(4): 1860-1869, Autumn 2025

RESEARCH PAPER

Green Synthesis of Iron Nanoparticles Using Propolis and Their In Vitro Antifungal Efficacy Against Trichophyton Fungi

*Hala M. Mutar [1], Hayder Kamil Jabber Al Kaabi [2], Baneen Najm Alhasanawi [3] and Ahmed Jassim Neama [4]**

[1] *Collage of Medicine, AL-Qadisiyah University, AL-Diwaniyah, Iraq*

[2] *Collage of Nursing, AL-Qadisiyah University, AL-Diwaniyah, Iraq*

[3] *Collage of Veterinary Medicine, AL-Qadisiyah University, AL-Diwaniyah, Iraq*

[4] *Collage of Biotechnology, AL-Qadisiyah University, AL-Diwaniyah , Iraq*

ARTICLE INFO

Article History:
Received 18 June 2025
Accepted 23 September 2025
Published 01 October 2025

Keywords:
Trichophyton
Iron nanoparticles
Propolis
Fungicidal

ABSTRACT

The increasing prevalence of dermatophytic infections caused by Trichophyton species highlights the urgent demand for safer and more effective antifungal therapies. In this study, iron nanoparticles (FeNPs) were synthesized through a green approach using methanolic Iraqi propolis extract as a natural reducing and stabilizing agent. The obtained FeNPs were characterized by UV–Vis. spectroscopy, field emission scanning electron microscopy (FESEM), Fourier-transform infrared spectroscopy (FTIR), and X-ray diffraction (XRD). The UV–Vis. spectrum exhibited a distinct absorption peak at approximately 280 nm, confirming nanoparticle formation, while FESEM analysis revealed irregular particles with an average size of 54.34 ± 1.22 nm. FTIR confirmed the presence of functional groups from propolis compounds, including O–H, C=O, and Fe–O, capping the nanoparticle surface. XRD patterns indicated the crystalline nature of the particles, with sizes ranging from 57 to 109 nm. Antifungal assays demonstrated a concentration-dependent inhibition of T. rubrum, with minimum inhibitory and fungicidal concentrations of 0.250 µg/mL and 2 µg/mL, respectively. Overall, propolis-capped FeNPs exhibited notable antifungal activity, combining the inherent antimicrobial properties of iron oxide and propolis to provide a promising, sustainable, and safer therapeutic alternative for resistant dermatophyte infections.

How to cite this article
Mutar H., Al Kaabi H., Alhasanawi B., Neama A. Green Synthesis of Iron Nanoparticles Using Propolis and Their In Vitro Antifungal Efficacy Against Trichophyton Fungi. J Nanostruct, 2025; 15(4):1860-1869. DOI: 10.22052/JNS.2025.04.033

INTRODUCTION

Dermatophyte infections caused by Trichophyton species are still considered a big problem for public health around the world [1]. In particular, the species Trichophyton rubrum is the leading causative agent of superficial dermatomycoses worldwide, which account for over 70% of all dermatophyte cases [2]. T. rubrum infections are characterized as chronic, resistant to most antifungal therapies, and a high likelihood of recurrence after treatment [3]. Recent reports have highlighted treatment-resistant T. rubrum dermatophytosis as an emerging threat, giving the limitations of current antifungal therapy [4].

The challenges associated with dermatophytic infections scored highly in warm, humid climates,

* *Corresponding Author Email: ahmed.neamah@qu.edu.iq*

including the Middle East [5]. In some Middle Eastern and Asian populations, the prevalence of cutaneous fungal infections exceeds 20% [6]. Recent estimates indicate that superficial fungal infections of the skin affect approximately 4.8% of Iraq's population (over two million people) [7]. Standard therapies for dermatophytosis, which include topical azoles, systemic terbinafine and other allylamines, are often protracted and not always curative [8, 9]. Prolonged therapeutic courses are required for tinea infections of nails and skin, yet clinical outcomes are limited by issues of patient non-compliance, drug toxicity, and the development of antifungal resistance [10]. These epidemiological and therapeutic challenges drive the search for new, more effective and safe antifungal strategies.

Nanotechnology-based strategies have emerged as promising therapeutic alternatives for combating fungal pathogens [11]. In particular, the metallic nanoparticles which have been reported in several studies to exhibit unique antimicrobial properties due to their high surface area and their capacity in generating reactive oxygen species (ROS) at the site of infection [12]. Green-synthesized metal nanoparticles (MNPs) derived from biological extracts display broad-spectrum antimicrobial efficacy [13]. For instance, biosynthesized iron nanoparticles demonstrate potent antifungal activity in vitro, achieving complete T. rubrum growth inhibition at targeted concentrations [14]. Nanoscale zero-valent iron has similarly demonstrated significant suppression of T. rubrum and other pathogenic fungi [15]. The therapeutic potential of these nano-formulations derives from their ability to disrupt fungal cell membrane integrity and trigger protein damage via ROS generation and metal ion release [16]. Investigations reveal that these materials deliver highly effective fungicidal activity even against strains resistant to conventional therapies [17]. In recent rodent studies, topically applied biosynthesized silver nanoparticles eliminated T. rubrum infections within two weeks [18].

These observations emphasize the potential of nanomaterials as novel therapeutic approaches for refractory superficial mycoses [19]. Propolis, a resinous Propolis contains rich concentrations of flavonoids, phenolic acids, and terpenes. Propolis is additionally recognized for its powerful antimicrobial and antifungal characteristics, employed in traditional medicine for centuries [20]. The chemical constituents of propolis facilitate metal ion reduction to nanoscale dimensions

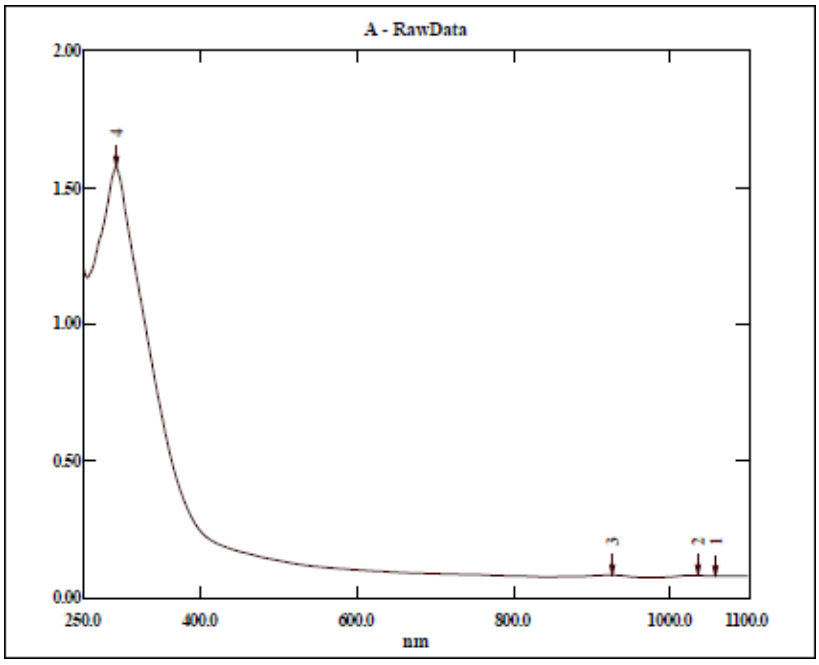

Fig. 1. UV-Vis Absorption Spectrum of Propolis-Synthesized Iron Nanoparticles.

while concurrently stabilizing the resulting nanoparticles [21]. This methodology has enabled the biosynthesis of diverse metal nanoparticles (Ag, Au, etc.) with superior biological attributes [22]. The combination of the intrinsic antifungal properties of propolis with the reactivity and the low toxicity of the iron can result in generating a very effective antimicrobial nanomaterial [23]. Such material offers a sustainable, eco-friendly, and safer solution to the emerging cases of highly resistant and recurrent dermatophyte infections [24].

This study assesses the in vitro antifungal efficacy of propolis-mediated iron nanoparticles against Trichophyton rubrum. The results will offer significant insights into the therapeutic prospects of propolis-synthesized iron nanoparticles as a novel treatment approach for dermatophytic infections.

MATERIALS AND METHODS

The study received approval from the Institutional Research Committee at the College of Veterinary Medicine, University of Al-Qadisiyah, Iraq, and was conducted between June 2024 and July 2025. Propolis samples were collected from active honeybee hives in Erbil, Iraq. The methanolic extract was prepared following Al-Khalaf et al. (2022) with minor modifications. Iron nanoparticles were synthesized using a green approach with Iraqi propolis serving as both reducing and capping agent. Characterization encompassed UV–Vis spectroscopy, FESEM, FTIR, and XRD, while antifungal efficacy against Trichophyton rubrum was evaluated through in vitro inhibition assays, MIC, and MFC determinations [25, 26] The chemicals utilized included local Iraqi propolis, methanol (analytical grade), iron(II) sulfate heptahydrate ($FeSO_4 \cdot 7H_2O$), Potato Dextrose Agar (PDA), Sabouraud Dextrose Broth (SDB), ketoconazole as standard antifungal control, and distilled water. The instruments employed comprised a UV–Vis spectrophotometer (1900, Shimadzu, Japan), field emission scanning electron microscope (MIRA III, Tescan, Czech Republic), Fourier-transform infrared spectrophotometer (1800, Shimadzu, Japan), X-ray diffractometer (Pw1730, Philips, Netherlands) with CuKα source (40 kV, 30 mA), centrifuge (13,000 rpm), incubator maintained at 28 °C, 96-well microtiter plates, and SPSS software version 27 for statistical analysis [27].

Propolis pieces were rinsed in methanol for seven days, filtered through Whatman No. 1 paper, and dried to obtain the extract. Iron nanoparticles were synthesized by mixing 2 mL of propolis extract with 20 mL of 13 mM $FeSO_4 \cdot 7H_2O$ solution (ratio 1:10) in a 100 mL Erlenmeyer flask. The solution was stirred for 8 h at 60–70 °C, followed by 24 h at 37 °C. Nanoparticle formation was indicated by the appearance of a black color. The nanoparticles were precipitated by centrifugation (13,000 rpm, 15 min) and stored at −4 °C. Characterization was conducted using UV–Vis (200–1100 nm), FESEM

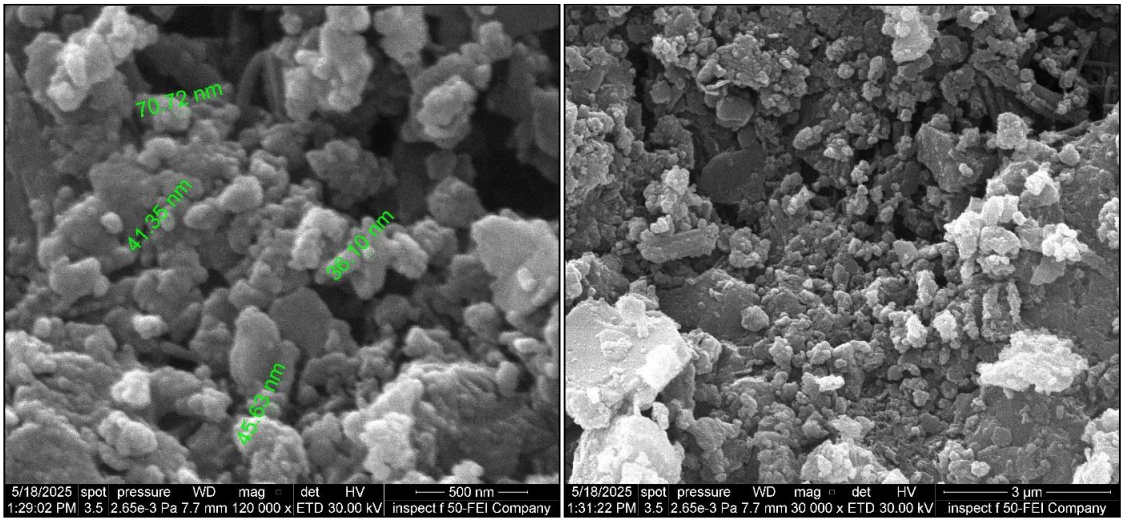

Fig. 2. Field Emission Scanning Electron Microscopy (FESEM) Image of Propolis-Synthesized Iron Nanoparticles.

(20 kV), FTIR, and XRD with the Scherrer formula for crystallite size estimation. For antifungal testing, T. rubrum was cultured on PDA at 28 °C for 7 days. Iron nanoparticles at different concentrations were incorporated into PDA and inoculated with fungal discs (5 mm). Positive controls contained fungus only, negative controls were fungus-free, and ketoconazole served as a reference. Growth inhibition was calculated by measuring colony diameters. MIC and MFC values were determined by microdilution in SDB with two-fold serial dilutions (0.065–32 µg/mL) and incubation at 28 °C for 7 days. The lowest concentrations showing no visible growth were recorded as MIC and MFC. All assays were performed in triplicate. Statistical analysis was conducted using one-way ANOVA with LSD, considering $p < 0.05$ as significant.

RESULTS AND DISCUSSION

As shown in the Fig. 1, the UV-Vis spectrum of the iron nanoparticles shows a prominent absorption peak at approximately 280 nm. The findings indicate a successful formation and presence of nanoparticles. The broad nature of this peak suggests a degree of particle size distribution, while the relatively low absorbance in the visible region (above 400 nm) indicates good dispersion and minimal aggregation.

The UV–Vis. spectrum of synthesized iron nanoparticles (Fe NPs) of the current study showed a strong absorption around 280 nm. The finding indicates a successful nanoparticle formation with a relatively extended size distribution. This observation is to some degree consistent with other reports of iron oxide nanomaterials. However, the exact peak positions were found to vary among studies. For example, one green synthesis study reported sharp UV–Vis peaks at ~290–300 nm for FeO and Fe_2O_3 nanoparticles [28]. The measured broad peak (at 280 nm) by the current analysis may reflect the small size of the particle formation or the capping molecules from propolis. Propolis extracts themselves exhibit UV absorption around 270–280 nm due to larger amounts of phenolic and flavonoid content[29]. This means some of the UV absorbance in our sample could arise from residual propolis compounds coating the nanoparticles. In a similar approach, selenium nanoparticles biosynthesized with propolis showed a strong UV–Vis band at ≈265 nm, attributed to the nanoparticle's plasmon and propolis polyphenols [29, 30].

It is worth noting that other iron oxide nanoparticle studies have sometimes reported a more red-shifted feature. Ukanwa et al. showed a broad SPR band between 350–400 nm for propolis-mediated Fe_2O_3 NPs [31]. In their case, a single broad band was associated with roughly spherical, larger particles. By comparison, the current 280 nm peak and low absorbance beyond 400 nm suggest well-dispersed, nano-sized particles with minimal aggregation, an indicator of effective capping and stabilization by propolis compounds.

Fig. 2 shows the FESEM image of the prepared

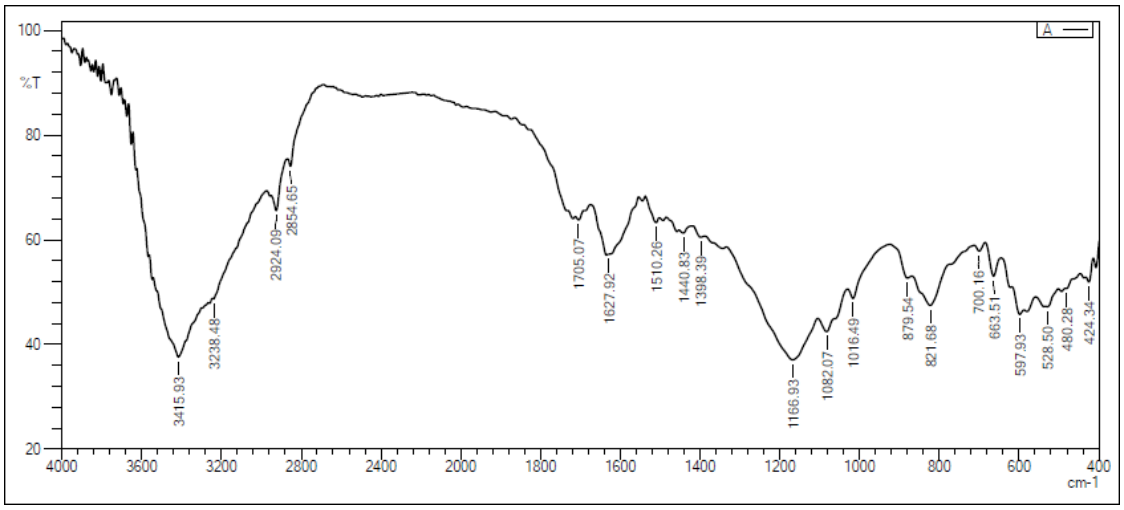

Fig. 3. FTIR Spectrum of Propolis-Synthesized Iron Nanoparticles.

iron nanoparticles which reveal irregularly shaped particles with varying nano sizes, with average particle size 54.34±1.22 for 100 particles. The surface appears rough and somewhat agglomerated, suggesting a tendency for the nanoparticles to cluster, which is common for highly reactive nanomaterials.

Imaging with FESEM revealed irregularly shaped iron nanoparticles with an average size of about 54 nm. This is prevalent in biosynthesized iron oxides owing to the adhesive characteristics of reactive surfaces and organic capping agents [32]. In fact, a similar green synthesis using Melia azedarach leaf extract produced Fe_3O_4 nanoparticles that appeared irregular in shape under SEM [33]. TEM analysis revealed primary particles averaging 50 nm in diameter, with clustering attributed to plant biomolecule coatings. This observation aligns with documented tendencies of nanoscale particles to form clusters [34]. Particle sizes from various green synthesis methods exhibit considerable variation across studies. The observed 54 nm average falls within the mid-range reported in existing literature [35]. Studies report varying particle sizes, with some documenting smaller dimensions and others larger ones. Ukanwa and Özgör, utilizing propolis extract, obtained considerably larger Fe_2O_3 nanoparticles averaging approximately 108 nm [31]. The smaller size nanoparticles in this study could be due to specific propolis components or to conditions yielding a higher nucleation rate [24]. All these studies, including ours, report some degree of agglomeration. This is likely because of the natural capping agents (like polyphenols in propolis or leaf extracts) which bind the particles together [31, 36]. Nonetheless, the overall nanoscale dimension is maintained throughout studies.

Fig. 3 displays the FTIR spectrum of iron nanoparticles, revealing several characteristic absorption bands. This analysis elucidates the surface chemistry and functional groups present, where a broad, intense band at approximately 3415 cm^{-1} alongside a smaller peak at 3238 cm^{-1} indicates O-H stretching vibrations. This is likely attributed to adsorbed water molecules on the nanoparticle surface and/or the presence of hydroxyl groups, which are considered as characteristic features for iron oxide nanoparticles. The peaks at 2924 cm^{-1} and 2854 cm^{-1} relate to C-H stretching vibrations suggest the presence of organic residues or capping agents from the synthesis procedure. The heist observed band at 1705 cm^{-1} can be related to the C=O stretching vibration of a carbonyl group. This band might originate from unreacted precursors, organic impurities, or carboxylic acid groups that

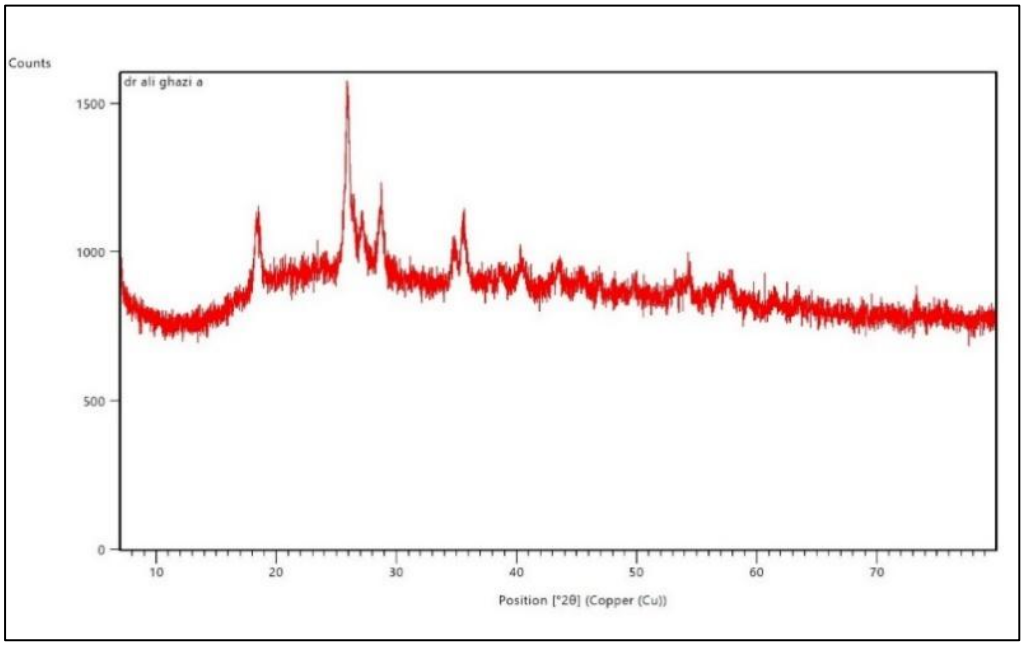

Fig. 4. X-ray Diffraction (XRD) Pattern of Propolis-Synthesized Iron Nanoparticles.

could be involved in the stabilization process. Bands observed around 1627 cm^{-1} (possibly C=C stretching or O-H bending of adsorbed water), and 1510 cm^{-1} and 1440 cm^{-1} (attributed to asymmetric and symmetric stretching of carboxylate groups (COO^-)), further support the presence of organic moieties on the nanoparticle surface. The region between 1200 cm^{-1} and 1000 cm^{-1} which showing peaks like 1166 cm^{-1}, 1082 cm^{-1}, and 1016 cm^{-1}, often points to C-O stretching vibrations of alcohols, ethers, or carbohydrates. The strong absorption bands around 597 cm^{-1}, 528 cm^{-1}, 480 cm^{-1} and 424 cm^{-1} are characteristic of Fe-O stretching vibrations from the iron oxide lattice. This finding confirms the successful formation of iron oxide nanoparticles.

The FTIR spectrum of the synthesized iron nanoparticles distinctly reveals multiple functional groups from the propolis capping matrix. A broad, intense O–H stretching band at approximately 3415 cm^{-1} indicates hydroxyl groups and adsorbed moisture. This characteristic is commonly observed in iron oxide nanoparticles stabilized with natural products [29]. Comparable results have been documented elsewhere. For example, propolis-mediated Se nanoparticles exhibited a broad O–H band at approximately 3400 cm^{-1} [24]. Plant-derived iron oxides typically exhibit O–H absorptions, which are expected to originate from residual water and phenolic compounds [37]. Analysis also showed distinct C–H stretching peaks at 2924 and 2854 cm^{-1}, suggesting presence of aliphatic hydrocarbons from organic residues or capping agents [38]. Consistently, researchers have found C–H stretches ~2950–2850 cm^{-1} in nanoparticles synthesized with propolis or plant extracts, attributing them to organic stabilizers (like lipids or lignin fragments) [29, 39]. The study also reported stretching C=O band at 1705 cm^{-1} suggests presence of carbonyl groups, which might be originated from esters, carboxylic acids, or unreacted aldehydes in propolis [40]. This is in line with other green-synthesized iron oxides, which often show a carbonyl band in the 1700–1740 cm^{-1} region [29]. Additional peaks at approximately 1627, 1510, and 1440 cm^{-1} correspond to aromatic C=C and carboxylate (COO^-) stretches, further confirming that organic acids from propolis bind to the particle surface. Comparable bands have been documented when biomolecules stabilize iron nanoparticles [4]. Importantly, it was observed C–O stretching

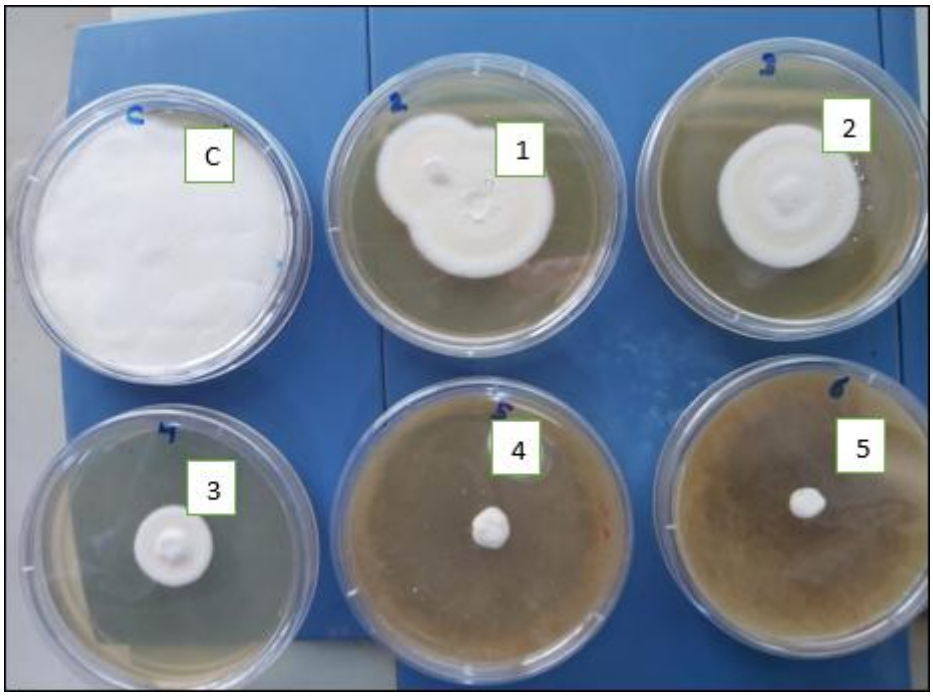

Fig. 5. Inhibitory Effect of Propolis-Synthesized Iron Nanoparticles on Trichophyton rubrum Growth in PDA Culture.

signals (1166, 1082, 1016 cm^{-1}) consistent with alcohols, ethers or polyols. This is likely originating from polyphenols and sugars present in propolis [41]. A study described propolis-capped Fe_2O_3 with several organic peaks than uncapped Fe_2O_3, confirming the coating by propolis compounds [31]. Finally, Fe–O lattice vibrations manifest as strong bands within the 600–400 cm^{-1} range, with observed peaks at 597, 528, 480, and 424 cm^{-1}. These represent characteristic signatures of iron–oxygen bonds in iron oxide structures. Literature supports this assignment, as bands near 550 cm^{-1} are consistently attributed to Fe–O stretching in iron oxides [4, 29]. In fact, our observed bands align well with standard ranges for magnetite or maghemite, where major Fe–O modes occur at ~540–580 cm^{-1} and ~430 cm^{-1} [42]. The presence of these bands in our samples definitively confirms the formation of iron oxide nanoparticles.

The X-ray Diffraction (XRD) pattern of the iron nanoparticles, as shown in Fig. 4, presents several well-defined diffraction peaks, strongly indicating a crystalline formation of the material rather than an amorphous structure. The X-ray diffraction (XRD) analysis of the nanoscale iron material reveals several well-defined diffraction peaks, indicating its crystalline nature. Significant peaks are observed at 2 theta positions of approximately 18.46°, 25.90°, 27.11°, 28.70°, 34.79°, 35.59°, 40.33°, 43.46°, 45.36°, 46.87°, and 54.25°. The broadness of these peaks suggests a nanocrystalline size for the iron particles. The varying intensities and relative intensities of these peaks suggest the presence of different crystallographic planes and potentially varying degrees of crystallinity or preferred orientation. The crystallite sizes range significantly from 57 nm to 109 nm, confirming the nanoscale nature of the material's crystalline domains.

X-ray diffraction of our iron nanoparticles (Fig. 4) revealed several well-defined Bragg peaks. Such findings suggest a crystalline iron oxide formation and not diffused amorphous material [43]. The 2θ positions we observed (approximately 18.46°, 25.90°, 27.11°, 28.70°, 34.79°, 35.59°, 40.33°, 43.46°, 45.36°, 46.87°, 54.25°, etc.) correspond to various crystallographic lattice of iron oxides (hematite or maghemite) [4, 44]. In fact, a study reported α-Fe_2O_3 (hematite) reflections at 24.1°, 33.2°, 35.1°, 40.9°, 49.5°, 54.1°, 57.5° (2θ) values quite close to many of our diffraction angles [4]. This suggests our sample may contain hematite (α-Fe_2O_3) as a major phase. A closer look at literature reveals that JCPDS card 33-0664 for α-Fe_2O_3 matches the XRD pattern of propolis-derived Fe_2O_3 in a recent study [45]. Another study identified a minor maghemite (γ-Fe_2O_3) peak at 2θ ≈ 30.7°, suggesting that secondary phases may coexist when employing natural extracts [46]. Collectively, multiple diffraction peaks with varying intensities suggest diverse crystallographic orientations and potentially mixed iron oxide polymorphs. These peaks exhibited relatively broad profiles, characteristic of nanocrystalline materials. Consequently, the Scherrer equation was employed to estimate crystallite domains, yielding sizes ranging from approximately 57 to 109 nm, consistent with nanoscale iron oxide dimensions [47]. Findings from XRD confirm the crystalline structure of the iron nanoparticles and these structures are in the nanometer size scale.

In vitro results demonstrated that iron nanoparticles exhibit substantial antifungal activity. Similar investigations revealed that green-synthesized iron oxide nanoparticles display efficacy against diverse pathogenic fungi [23, 48, 49]. For example, a study by Parveen et al. examined green-synthesized Fe_2O_3 nanoparticles

Table 1. Effect of different concentrations of iron nanoparticles on the trichophyton growth in culture media.

Concentration (µg/mL)	Mean± SE of Inhibition percentage
25	43.54±2.38^{d}
50	54.35±1.76^{c}
100	81.98±2.66^{b}
200	93.69±3.13^{a}
400	94.29±2.94^{a}
Amphotericin	96.58±2.12^{a}
LSD(p<0.05)	3.081

*Different letters between any two means denote to the significant difference

Table 2. Minimum Inhibitory Concentration (MIC) and Minimum Fungicidal Concentration (MFC) of Propolis-Synthesized Iron Nanoparticles Against Trichophyton rubrum.

Concentration(µg/ml)	0.065	0.125	0.250	0.500	1	2	4	8	16	32
MIC value	+	+	–	–	–	–	–	–	–	–
MBC value	+	+	+	+	+	+	–	–	–	–

(+) positive growth (-) No growth

against several phytopathogenic and spoilage fungi [50]. The study found broad-spectrum antifungal efficacy with considerably high inhibition zones. Current results align with these previous reports and strongly indicating that iron oxide nanoparticles can be very effective against fungal growth [51]. Likewise, iron oxide nanoparticles were potent against dermatophytes, such as T. mentagrophytes and T. verrucosum, which are responsible for various types of skin infections in animals [52].

The addition of propolis as a reducing or as capping agent may effectively improve the antimicrobial potency of these nanoparticles [53]. Propolis is well-documented fungal and bacterial growth inhibitor for its richness in flavonoids and phenolic acids that are widely used as antifungal agents [54]. In this study, the propolis-capped Fe NPs showed higher activity against fungal growth compared to free-Fe NPs. Similar studies compared plain Fe_2O_3 NPs to propolis-capped Fe_2O_3 and found the latter to be more active against fungus [31]. Moreover, converting propolis into nanoparticles would essentially increase efficacy by enhancing bioavailability, improving cellular uptake, and enabling targeted delivery [53, 55]. The combined effect of the iron oxide core and the external propolis coat could explain the robust antifungal activity that has been observed by the current investigation [49]. Furthermore, the MIC of propolis-capped Fe_2O_3 is estimated at tens of micrograms per milliliter, which is clinically acceptable for a treatment approach. However, further optimization is required to minimize potential cytotoxicity and enhance efficacy for use as next-generation antifungal agents.

CONCLUSION

This study successfully demonstrated the green synthesis of iron nanoparticles using methanolic Iraqi propolis extract as a natural reducing and stabilizing agent. The synthesized FeNPs were well-characterized, showing a distinct absorption peak at ~280 nm in UV–Vis spectra, irregular morphology with an average size of 54.34 ± 1.22 nm by FESEM, the presence of key functional groups such as O–H, C=O, and Fe–O through FTIR analysis, and a crystalline structure with sizes ranging from 57 to 109 nm confirmed by XRD. Biological evaluation revealed a concentration-dependent inhibition of Trichophyton rubrum, with MIC and MFC values of 0.250 µg/mL and 2 µg/mL, respectively, highlighting their strong antifungal potential. The integration of propolis as both a reducing and capping agent not only stabilized the nanoparticles but also enhanced their antifungal properties through its bioactive phenolic and flavonoid content. These findings emphasize the promise of propolis-mediated iron nanoparticles as a sustainable, eco-friendly, and safer alternative to conventional antifungal drugs, especially against resistant dermatophyte infections. However, further in vivo investigations and cytotoxicity assessments are essential to validate their clinical applicability and to optimize their use as next-generation antifungal agents.

CONFLICT OF INTEREST

The authors declare that there is no conflict of interests regarding the publication of this manuscript.

REFERENCES

1. Chanyachailert P, Leeyaphan C, Bunyaratavej S. Cutaneous Fungal Infections Caused by Dermatophytes and Non-Dermatophytes: An Updated Comprehensive Review of Epidemiology, Clinical Presentations, and Diagnostic Testing. Journal of Fungi. 2023;9(6):669.
2. Kruithoff C, Gamal A, McCormick TS, Ghannoum MA. Dermatophyte Infections Worldwide: Increase in Incidence and Associated Antifungal Resistance. Life. 2023;14(1):1.
3. Gupta AK, Elewski B, Joseph WS, Lipner SR, Daniel CR, Tosti A, et al. Treatment of onychomycosis in an era of antifungal resistance: Role for antifungal stewardship and topical antifungal agents. Mycoses. 2024;67(1).
4. Hwang JK, Bakotic WL, Gold JAW, Magro CM, Lipner SR. Isolation of Terbinafine-Resistant Trichophyton rubrum from Onychomycosis Patients Who Failed Treatment at an Academic Center in New York, United States. Journal of Fungi. 2023;9(7):710.
5. Hill RC, Caplan AS, Elewski B, Gold JAW, Lockhart SR,

Smith DJ, et al. Expert Panel Review of Skin and Hair Dermatophytoses in an Era of Antifungal Resistance. Am J Clin Dermatol. 2024;25(3):359-389.
6. Xihua Y, Xiaofeng Q, Lulu T, Zhiyu K, Min D, Yi W. Fungal Skin Disease Incidence, Prevalence and Disability-Adjusted Life Years in Four Asian Countries (1990–2019). Mycoses. 2025;68(2).
7. Mohammad KA, Ismail HM, Shekhany KAM, Yashooa RK, Younus DA, Abdullah SK, et al. Fungal disease incidence and prevalence in Iraq – Preliminary estimates. J Medical Mycology. 2024;34(4):101516.
8. Sonego B, Corio A, Mazzoletti V, Zerbato V, Benini A, di Meo N, et al. Trichophyton indotineae, an Emerging Drug-Resistant Dermatophyte: A Review of the Treatment Options. Journal of Clinical Medicine. 2024;13(12):3558.
9. Nenoff P, Klonowski E, Uhrlaß S, Schaller M, Paasch U, Mayser P. Topische und systemische antimykotische Behandlung von Dermatomykosen. Die Dermatologie. 2024;75(8):655-673.
10. Koh XQ, Pan JY. Recalcitrant cutaneous fungal infections—A growing problem. Australas J Dermatol. 2023;64(3):315-321.
11. de Almeida Campos L, Fin MT, Santos KS, de Lima Gualque MW, Freire Cabral AKL, Khalil NM, et al. Nanotechnology-Based Approaches for Voriconazole Delivery Applied to Invasive Fungal Infections. Pharmaceutics. 2023;15(1):266.
12. Wahab S, Salman A, Khan Z, Khan S, Krishnaraj C, Yun S-I. Metallic Nanoparticles: A Promising Arsenal against Antimicrobial Resistance—Unraveling Mechanisms and Enhancing Medication Efficacy. Int J Mol Sci. 2023;24(19):14897.
13. Maťátková O, Michailidu J, Miškovská A, Kolouchová I, Masák J, Čejková A. Antimicrobial properties and applications of metal nanoparticles biosynthesized by green methods. Biotechnol Adv. 2022;58:107905.
14. Haris M, Fatima N, Iqbal J, Chalgham W, Mumtaz AS, El-Sheikh MA, et al. Oscillatoria limnetica Mediated Green Synthesis of Iron Oxide (Fe_2O_3) Nanoparticles and Their Diverse In Vitro Bioactivities. Molecules. 2023;28(5):2091.
15. Obaid HS, Halbus AF. Boosting iron oxide nanoparticles activity for dyes removal and antifungal applications by modifying its surface with polyelectrolytes. Chemical Physics Impact. 2023;6:100244.
16. Ahuja A, Bajpai M. Nanoformulations Insights: A Novel Paradigm for Antifungal Therapies and Future Perspectives. Curr Drug Del. 2024;21(9):1241-1272.
17. Jangjou A, Zareshahrabadi Z, Abbasi M, Talaiekhozani A, Kamyab H, Chelliapan S, et al. Time to Conquer Fungal Infectious Diseases: Employing Nanoparticles as Powerful and Versatile Antifungal Nanosystems against a Wide Variety of Fungal Species. Sustainability. 2022;14(19):12942.
18. Abdallah BM, Rajendran P, Ali EM. Potential Treatment of Dermatophyte Trichophyton rubrum in Rat Model Using Topical Green Biosynthesized Silver Nanoparticles with Achillea santolina Extract. Molecules. 2023;28(4):1536.
19. Chaudhari V, Vairagade V, Thakkar A, Shende H, Vora A. Nanotechnology-based fungal detection and treatment: current status and future perspective. Naunyn-Schmiedeberg's Arch Pharmacol. 2023;397(1):77-97.
20. Javed S, Mangla B, Ahsan W. From propolis to nanopropolis: An exemplary journey and a paradigm shift of a resinous substance produced by bees. Phytother Res. 2022;36(5):2016-2041.
21. Zullkiflee N, Taha H, Usman A. Propolis: Its Role and Efficacy in Human Health and Diseases. Molecules. 2022;27(18):6120.
22. Venkata ALK, Sivaram S, M S, P M S, Srilakshman G, Muthuraman MS. Review on terpenoid mediated nanoparticles: significance, mechanism, and biomedical applications. Advances in Natural Sciences: Nanoscience and Nanotechnology. 2022;13(3):033003.
23. Rezk N, Abdelsattar AS, Makky S, Hussein AH, Kamel AG, El-Shibiny A. New formula of the green synthesised Au@Ag core@shell nanoparticles using propolis extract presented high antibacterial and anticancer activity. AMB Express. 2022;12(1).
24. Zúñiga-Miranda J, Guerra J, Mueller A, Mayorga-Ramos A, Carrera-Pacheco SE, Barba-Ostria C, et al. Iron Oxide Nanoparticles: Green Synthesis and Their Antimicrobial Activity. Nanomaterials. 2023;13(22):2919.
25. Barsola B, Kumari P. Green synthesis of nano-propolis and nanoparticles (Se and Ag) from ethanolic extract of propolis, their biochemical characterization: A review. Green Processing and Synthesis. 2022;11(1):659-673.
26. Al-Khalaf AA, Alabdelkareem I, Al-Rejaie SS, Mohany M, Hozzein WN. Molecular Docking Studies on Methanolic Propolis Extracts Collected from Different Regions in Saudi Arabia as a Potential Inhibitor of Topoisomerase IIβ. Separations. 2022;9(12):392.
27. Moustafa M, shams Al Din R. green synthesis and characterization of iron-oxide nanoparticles by guava aqueous leaves extract for doxorubicin drug loading. Journal of Bioscience and Applied Research. 2017;3(4):177-180.
28. Monshi A, Foroughi MR, Monshi MR. Modified Scherrer Equation to Estimate More Accurately Nano-Crystallite Size Using XRD. World Journal of Nano Science and Engineering. 2012;02(03):154-160.
29. Xue P, Yang X, Sun X, Ren G. Antifungal activity and mechanism of heat-transformed ginsenosides from notoginseng against Epidermophyton floccosum, Trichophyton rubrum, and Trichophyton mentagrophytes. RSC Advances. 2017;7(18):10939-10946.
30. Yekeen MO, Ibrahim M, Wachira J, Pramanik S. Green Synthesis and Characterization of Iron Oxide Nanoparticles Using Egeria densa Plant Extract. Applied Biosciences. 2025;4(2):27.
31. R S, M M, Yogananda Murthy VN. Biosynthesis and Characterization, Antioxidant and Antimicrobial Activities of Selenium Nanoparticles from Ethanol Extract of Bee Propolis. Journal of Nanomedicine and Nanotechnology. 2019;10(01).
32. Wali AT. Biosynthesis, Characterization and Bioactivity of Selenium Nanoparticles Synthesized by Propolis. The Iraqi Journal of Veterinary Medicine. 2019;43(1):197-209.
33. Sunday U, Erkay zg r SU, Erkay zg r. Synthesis of Iron oxide Nanoparticle using Propolis from Northern Cyprus and Evaluation of its Antibacterial, Anticancer Potential on MDA-MB 231 cells. J Chem Soc Pak. 2023;45(4):336-336.
34. Mahdavi M, Namvar F, Ahmad M, Mohamad R. Green Biosynthesis and Characterization of Magnetic Iron Oxide (Fe_3O_4) Nanoparticles Using Seaweed (Sargassum muticum) Aqueous Extract. Molecules. 2013;18(5):5954-5964.
35. Abolarinwa TO, Ajose DJ, Oluwarinde BO, Montso KP, Fri J, Fayemi OE, et al. Antimicrobial Properties and Cytotoxicity of Iron Oxide Nanoparticles Synthesized Using Melia

azedarach Leaf Extract Against Diarrhoeal Pathogens. BioNanoScience. 2024;14(5):5003-5016.
36. Li C-W, Merlitz H, Sommer J-U. Scaling Behaviors of Nanoparticle Clusters That Are Driven through Brush-Decorated Nanopores. Macromolecules. 2023;56(21):8710-8720.
37. Yassin MT, Al-Otibi FO, Al-Askar AA, Alharbi RI. Green Synthesis, Characterization, and Antifungal Efficiency of Biogenic Iron Oxide Nanoparticles. Applied Sciences. 2023;13(17):9942.
38. Khairunnisa S, Wonoputri V, Samadhi TW. Effective Deagglomeration in Biosynthesized Nanoparticles: A Mini Review. IOP Conference Series: Materials Science and Engineering. 2021;1143(1):012006.
39. Franco RT, Silva AL, Licea YE, Serna JDP, Alzamora M, Sánchez DR, et al. Green Synthesis of Iron Oxides and Phosphates via Thermal Treatment of Iron Polyphenols Synthesized by a Camellia sinensis Extract. Inorganic Chemistry. 2021;60(8):5734-5746.
40. Kabeya JK, Ngombe NK, Mutwale PK, Safari JB, Matlou GG, Krause RWM, et al. Antimicrobial capping agents on silver nanoparticles made via green method using natural products from banana plant waste. Artificial Cells, Nanomedicine, and Biotechnology. 2025;53(1):29-42.
41. Hajizadeh YS, Harzandi N, Babapour E, Yazdanian M, Ranjbar R. Green Synthesize and Characterization of Copper Nanoparticles Using Iranian Propolis Extracts. Advances in Materials Science and Engineering. 2022;2022:1-9.
42. Abdullah NA, Zullkiflee N, Zaini SNZ, Taha H, Hashim F, Usman A. Phytochemicals, mineral contents, antioxidants, and antimicrobial activities of propolis produced by Brunei stingless bees Geniotrigona thoracica, Heterotrigona itama, and Tetrigona binghami. Saudi J Biol Sci. 2020;27(11):2902-2911.
43. Lima ABSd, Batista AS, Santos MRC, Rocha RdSd, Silva MVd, Ferrão SPB, et al. Spectroscopy NIR and MIR toward predicting simultaneous phenolic contents and antioxidant in red propolis by multivariate analysis. Food Chem. 2022;367:130744.
44. Sainz-Menchón M, González de Arrieta I, Echániz T, Nader K, Insausti M, Canizarès A, et al. Quantifying lattice vibrational modes and optical conductivity in mixed magnetite–maghemite nanoparticles. Physical Chemistry Chemical Physics. 2025;27(16):8498-8509.
45. Aich D, Samanta PK, Saha S, Kamilya T. Synthesis and Characterization of Super Paramagnetic Iron Oxide Nanoparticles. Nanoscience and Nanotechnology-Asia. 2020;10(2):123-126.
46. Qureshi AA, Javed S, Javed HMA, Jamshaid M, Ali U, Akram MA. Systematic Investigation of Structural, Morphological, Thermal, Optoelectronic, and Magnetic Properties of High-Purity Hematite/Magnetite Nanoparticles for Optoelectronics. Nanomaterials. 2022;12(10):1635.
47. Sharmila M, Mani RJ, Parvathiraja C, Kader SMA, Siddiqui MR, Wabaidur SM, et al. Photocatalytic Dye Degradation and Bio-Insights of Honey-Produced α-Fe2O3 Nanoparticles. Water. 2022;14(15):2301.
48. T SJK, V.R A, M V, Muthu A. Biosynthesis of multiphase iron nanoparticles using Syzygium aromaticum and their magnetic properties. Colloids Surf Physicochem Eng Aspects. 2020;603:125241.
49. Kushwaha P, Chauhan P. Microstructural evaluation of iron oxide nanoparticles at different calcination temperature by Scherrer, Williamson-Hall, Size-Strain Plot and Halder-Wagner methods. Phase Transitions. 2021;94(10):731-753.
50. Jamzad M, Kamari Bidkorpeh M. Green synthesis of iron oxide nanoparticles by the aqueous extract of Laurus nobilis L. leaves and evaluation of the antimicrobial activity. Journal of Nanostructure in Chemistry. 2020;10(3):193-201.
51. Abbas HS, Krishnan A. Magnetic Nanosystems as a Therapeutic Tool to Combat Pathogenic Fungi. Advanced Pharmaceutical Bulletin. 2020;10(4):512-523.
52. Parveen S, Wani AH, Shah MA, Devi HS, Bhat MY, Koka JA. Preparation, characterization and antifungal activity of iron oxide nanoparticles. Microb Pathog. 2018;115:287-292.
53. Ali MA, Ahmed T, Wu W, Hossain A, Hafeez R, Islam Masum MM, et al. Advancements in Plant and Microbe-Based Synthesis of Metallic Nanoparticles and Their Antimicrobial Activity against Plant Pathogens. Nanomaterials. 2020;10(6):1146.
54. Mukherje M. In Vitro Antimicrobial Activity of Polyacrylamide Doped Magnetic Iron Oxide Nanoparticles. International Journal of Materials, Mechanics and Manufacturing. 2014:64-66.
55. Afrasiabi S, Pourhajibagher M, Chiniforush N, Bahador A. Propolis nanoparticle enhances the potency of antimicrobial photodynamic therapy against Streptococcus mutans in a synergistic manner. Sci Rep. 2020;10(1).
56. Petruzzi L, Rosaria Corbo M, Campaniello D, Speranza B, Sinigaglia M, Bevilacqua A. Antifungal and Antibacterial Effect of Propolis: A Comparative Hit for Food-Borne Pseudomonas, Enterobacteriaceae and Fungi. Foods. 2020;9(5):559.